

# Lorentz Violations and the Casimir Effect

Sam Christensen

*Physics Department, California Polytechnic State University, San Luis Obispo, California 93407, USA*

(Dated: December 10, 2021)

## I. INTRODUCTION: WHY LORENTZ VIOLATIONS?

Most people, whether they are part of the scientific community or not, have likely heard of Albert Einstein and the theory of relativity. Relativity brought a new model of physics that with quantum mechanics it is thought to describe most natural phenomena. Einstein's General relativity offers a description of the relationship between the concepts of space and time as well as forces and accelerations while quantum mechanics and the standard model of particle physics deals directly with the probabilistic properties of subatomic particles. However, as most scientists will recall there are some key disagreements between Einstein's general relativity and quantum mechanics. General relativity describes things that are smooth and continuous while quantum mechanics describes objects and quantities that are quantized and discrete. This creates problems in a number of physical scenarios. The disagreement between these theories has led physicists to conclude that one of the two is incomplete. In an effort to write a quantum theory of gravity, string theory was developed. An anisotropy, or a direction dependent change of properties in a material, in particular string theory models led Professor Alan Kostelečký of Indiana University to develop the Standard Model Extension. This Standard Model Extension suggested that the central underlying mathematical concept of relativity, Lorentz symmetry, could be violated. Lorentz symmetry is a postulate of relativity stating that the laws of physics do not change depending on one's reference frame. That is, non-accelerating observers of a physical system should see the same physics play out regardless of their reference point. While this symmetry is often considered to be upheld, subsequent calculations suggested that it may be a broken symmetry suggesting physics beyond the standard model. Typically there are two types of symmetry that people consider. There is spontaneous symmetry breaking which means that symmetry is only broken in the vacuum state and there is explicit symmetry breaking in which the equations of motion of a system are described in a way that do not respect the symmetry. In our research we investigated the effects that an explicitly broken symmetry has on a system of photons between two parallel conducting plates in vacuum due to a physical phenomenon known as the Casimir effect.

The Casimir effect, first predicted by physicist Hendrik Casimir in 1948, describes the force that arises from imposing boundary conditions on a confined space due to fluctuations in the quantum vacuum. Unlike a classical vacuum, which is totally void of all particles, quantum field theory tells us that virtual particles are constantly being created and annihilated in a quantum vacuum. Virtual particles are temporary particle like fluctuations of the amount of energy at a point in space. The existence of this is corroborated by Heisenberg's uncertainty principle. This leads to a vacuum with a non-zero energy created by these virtual particles. For us, the virtual particle that we want to focus on are photons because of the rules that they must obey as electromagnetic waves. This is important for us when considering the aforementioned confined space and its boundary conditions. In our case, the confined space was the region between two parallel conducting plates. Here "conducting" is a key attribute as it describes how our virtual photons will behave in the presence of the plates. From electromagnetism, the electric field inside of a conductor is always zero. This means that the wave function of each virtual photon between the plates must go to zero as well because they are electromagnetic waves. When visualizing these wave functions it may be helpful to think of them as strings (string as in a piece of twine, no relation to string theory) stretching over all space that can be fixed depending on circumstance. When we say that the wave function of a particular photon goes to zero in a conductor this means that we are choosing to fix one of its ends at zero inside that conductor, much like clipping a string to a wall. Now considering that we have two parallel plates, this means different things for photons between the plates and photons outside of the plates. Between the two plates we have photons that are "fixed" at both ends in the direction perpendicular to the plates. While the wave functions are zero in the plates, they may have an integer number of nodes (bumps or peaks and troughs) between them. This is like having a string fixed on both ends, like a guitar, and noticing that the only exact integer numbers of wavelengths appear. When one end of the guitar string is unfastened however, we may wiggle the entire string however we please and will see any number of wavelengths and potentially different wavelengths across the same string. This is characteristic of photons outside of the plates. In other words, the photons outside the plates may take on any real number of wavelengths. So, we have only integer numbers of wavelengths allowed between the plates with real numbers of wavelengths allowed outside the plates. At first this seems as if we have reached a dead end. We know that there are an infinite number of integers as well as an infinite number of real numbers. So, at first glance it appears that the total energy of the system will just be infinite and there is nothing left to calculate. However, from set theory we know that the cardinality of the natural numbers is infinite yet smaller than the also infinite cardinality of the real numbers. It is in the difference between these two "sizes" of

infinity that we can find a potentially meaningful quantity to calculate. The reference point for energy in a system can always be chosen, just so long as the other energies are also defined with respect to the same reference point. So, we don't need to worry about this seemingly infinite amount of energy if we can calculate the difference between the vacuum energy between the plates and the vacuum energy outside of the plates. To find this difference we want to take the infinite discrete sum of just the energies of the photons allowed between the two plates and subtract off the background. This is typically done with a physical interpretation of the Riemann Zeta function, but as this method is often not justified in tests, we proved its equivalence to the Euler-Maclaurin sum-integral formula describing the difference between continuous and discrete sums. This is actually quite interesting that a concept typically exclusive to number theory takes on a physical significance. The calculation with Lorentz symmetry preserved is well known. As photons are massless particles, the traditional Einstein dispersion relation gives the following relationship between the energy and momentum,

$$E^2 = (\vec{p})^2 \quad (1)$$

For simplicity in the calculations it is standard to assume  $\hbar = c = 1$ . This means as the energy of a photon is given by  $E = \hbar\omega$  and the momentum of a photon is given by  $\vec{p} = \hbar\vec{k}$  for angular frequency  $\omega$  and wave number  $\vec{k}$  we may write,

$$\omega^2 = \vec{k}^2 \quad (2)$$

This gives us a good enough start to begin considering the case of a spacetime anisotropy.

## II. LORENTZ VIOLATING RESULT FOR THE CASIMIR EFFECT

From Kostelečký and Mewes 2008 paper equation (4),

$$p(\omega) \approx [1 + \sigma^0 \mp \sqrt{(\sigma^1)^2 + (\sigma^2)^2 + (\sigma^3)^2}] \omega \quad (3)$$

where  $p$  and  $\omega$  are the momentum and frequency respectively.[3] This is the adjusted form of equation 2 adjusted for Lorentz-violating terms from the Standard Model Extension. Each  $\sigma^{n'}$  represents a different combination of coefficients for Lorentz violation. Here we will say  $\sigma^{n'}$ 's are small so all of the squared terms under the radical will be very small and will go to zero in the limit. From there we can rename  $\sigma^0$  as simply  $\sigma$ .

$$|\vec{p}| = (1 + \sigma)\omega \quad (4)$$

We may next substitute  $\vec{p} = \vec{k}$  where  $\vec{k}$  is the wave vector and  $\vec{p} = \hbar\vec{k}$  as  $\hbar = c = 1$  and divide our expression over.

$$\omega = \frac{1}{1 + \sigma} |\vec{k}| \quad (5)$$

As mentioned before we consider  $\sigma$  to be small thus the fractional term in front of the wave number magnitude may be binomial expanded to the first order.

$$\omega = (1 - \sigma) |\vec{k}| \quad (6)$$

Now from Kostelečký and Mewes 2008 paper equation (5) we may substitute an expression of summed spherical harmonics for  $\sigma$ . This is given by equation (45) from the appendix. Here  $d$  is the dimension of a Lorentz violating operator and  $j, m$  are the indices of spherical harmonics in the sum with  $j \leq d - 2$ . In our research we ruled out cases with birefringence. This is the property that would change the behavior and properties of our photons depending on polarization. Instead we were simply interested in cases with translation directional dependence. From Kostelečký and Mewes 2008 this rules out all  $d$  except for  $d \geq 6$  and is even. This tells us that  $d - 4$  from the exponent of  $\omega$  is a positive even number.[3]

$$\omega = |\vec{k}| \left( 1 - \sum_{djm} \omega^{d-4} Y_{jm}(\hat{k}) C_{djm} \right) \quad (7)$$

In our new expression it is the  $C_{djm}$ 's that are small. So if we consider  $\omega^2$  and consider that small squared terms must go to zero we see that  $\omega^2 = \vec{k}^2$ . So as we know that  $d - 4$  is at least 2 then we may write  $\omega = |\vec{k}|$  inside the  $\omega$  term

with that power.

$$\omega = |\vec{k}| - \sum_{djm} |\vec{k}|^{d-3} Y_{jm}(\hat{k}) C_{djm} \quad (8)$$

Because of the zero-point energies of the photons allowed between the plates, we model the system as many harmonic oscillator in their ground states but of varying frequency. Summing over the ground states of these oscillators gives a total energy of  $E = \frac{1}{2} \sum \omega$ . So,

$$E = \frac{1}{2} \sum_{k_x k_y k_z} \omega \quad (9)$$

Where  $\sum_{k_x k_y k_z}$  is a triple sum over the components of the wave vector. Each frequency can be described by a number of different wave vectors so, this is necessary. We can then substitute for the  $k_x$  and  $k_y$  sums using the discrete sum to integral transformation in equation (47) with square plate side length  $L$ . We can do this in the  $x$  and  $y$  directions but not in  $z$  as the separation between the plates is oriented along this direction imposing the discrete wavelength condition.

$$E = \frac{1}{2} \sum_{k_z} \left(\frac{L}{2\pi}\right)^2 \int \int dk_x dk_y \omega \quad (10)$$

By dividing by the area of the plates  $L^2$  we obtain an expression for energy density on the plates  $\epsilon$ .

$$\epsilon = \frac{1}{8\pi^2} \sum_{k_z} \int \int dk_x dk_y \omega \quad (11)$$

We may now use the expression for Lorentz-violating photon frequency solved for in equation (8) to write our complete energy density sum.

$$\epsilon = \frac{1}{8\pi^2} \sum_{k_z} \int \int dk_x dk_y (|\vec{k}| - \sum_{djm} |\vec{k}|^{d-3} Y_{jm}(\hat{k}) C_{djm}) \quad (12)$$

By properties of integration and discrete summation, we may sum over both terms independently. The  $|\vec{k}|$  term is the sum for the Lorentz Invariant case which is well known. So instead we will just sum over  $\sum_{djm}$  term. As this term contains the corrections for Lorentz violations we will name it's corresponding correction to the energy density  $\delta\epsilon$ .

$$\delta\epsilon = -\frac{1}{8\pi^2} \sum_{k_z} \int \int dk_x dk_y \sum_{djm} |\vec{k}|^{d-3} Y_{jm}(\hat{k}) C_{djm} \quad (13)$$

We may once again sum each term independently and break up the  $\sum_{djm}$ . We do this by evaluating a general term holding  $d, j$  and  $m$  constant.

$$\delta\epsilon = -\frac{1}{8\pi^2} \sum_{k_z} \int \int dk_x dk_y |\vec{k}|^{d-3} Y_{jm}(\hat{k}) C_{djm} \quad (14)$$

This triple sum over the spherical harmonics is difficult to evaluate by component in its current form. Instead using equation (46), from the Mewes and Ledesma Tensor paper, we may write these spherical harmonics in terms of a spin basis  $k_\uparrow, k_\downarrow, k_z$  where  $k_\uparrow = \frac{1}{\sqrt{2}}(k_x + ik_y)$ ,  $k_\downarrow = \frac{1}{\sqrt{2}}(k_x - ik_y)$ . and  $k_z$  remains as we had it.[5]

$$\delta\epsilon = -\frac{C_{djm}}{8\pi^2} \sum_{k_z} \int \int dk_x dk_y |\vec{k}|^{d-3} (-\text{sgn}(m))^m \sqrt{\frac{(2j+1)(j+m)!(j-m)!}{4\pi 2^{|m|}}} \sum_{q|jm} \frac{\hat{k}_\uparrow^\alpha \hat{k}_\downarrow^\beta \hat{k}_z^\gamma}{2^{\min(\alpha,\beta)} \alpha! \beta! \gamma!} \quad (15)$$

Rearrange and name  $\chi = -\frac{C_{dim}}{8\pi^2}(-sgn(m))^m \sqrt{\frac{(2j+1)(j+m)!(j-m)!}{4\pi^2|m|}}$  consolidating the constants for now and making the overall expression a bit more wieldy.

$$\delta\varepsilon = \chi \sum_{k_z} \int \int dk_x dk_y |\vec{k}|^{d-3} \sum_{q|jm} \frac{k_{\uparrow}^{\alpha} k_{\downarrow}^{\beta} k_z^{\gamma}}{2^{\min(\alpha,\beta)} \alpha! \beta! \gamma! |\vec{k}|^{\alpha+\beta+\gamma}} \quad (16)$$

Remember that we may write  $k_x = \kappa \cos(\theta)$  and  $k_y = \kappa \sin(\theta)$  for some  $\kappa = k_x^2 + k_y^2$ . Using these knew coordinate definitions we may use the transformation and properties from array (48) and equation (49) to rewrite the double integral in polar coordinates of the x-y plane. We also have  $\alpha + \beta + \gamma = j$  for the  $q$  sum.[5]

$$\delta\varepsilon = \chi \sum_{k_z} \int \int \kappa d\kappa d\theta |\vec{k}|^{d-3} \sum_{q|jm} \left(\frac{1}{\sqrt{2}}\right)^{\alpha+\beta} \frac{e^{i\theta(\alpha-\beta)} \kappa^{\alpha+\beta} k_z^{\gamma}}{2^{\min(\alpha,\beta)} \alpha! \beta! \gamma! |\vec{k}|^j} \quad (17)$$

As mentioned previously, the periodic boundary conditions are imposed in the z-direction. Integer numbers of half-wavelengths describe the photons allowed between the plates, so we may write  $k_z = (\frac{n\pi}{a})$  for integer  $n$  and plate separation  $a$ .

$$\delta\varepsilon = \chi \sum_n \int \int \kappa d\kappa d\theta |\vec{k}|^{d-3} \sum_{q|jm} \left(\frac{1}{\sqrt{2}}\right)^{\alpha+\beta} \frac{e^{i\theta(\alpha-\beta)} \kappa^{\alpha+\beta} \left(\frac{n\pi}{a}\right)^{\gamma}}{2^{\min(\alpha,\beta)} \alpha! \beta! \gamma! |\vec{k}|^j} \quad (18)$$

We may then pull the factors independent of the integration through the integrals and separate the integration by dependence.

$$\delta\varepsilon = \chi \sum_n \sum_{q|jm} \left(\frac{1}{\sqrt{2}}\right)^{\alpha+\beta} \frac{\left(\frac{n\pi}{a}\right)^{\gamma}}{2^{\min(\alpha,\beta)} \alpha! \beta! \gamma!} \int_0^{2\pi} d\theta e^{i\theta(\alpha-\beta)} \int \kappa d\kappa (\kappa^{\alpha+\beta} |\vec{k}|^{d-j-3}) \quad (19)$$

Evaluating the integral in  $\theta$  we see that it is in fact the integral definition of the kronecker delta function multiplied by a factor of  $2\pi$ .

$$\delta\varepsilon = \chi \sum_n \sum_{q|jm} \left(\frac{1}{\sqrt{2}}\right)^{\alpha+\beta} \frac{\left(\frac{n\pi}{a}\right)^{\gamma}}{2^{\min(\alpha,\beta)} \alpha! \beta! \gamma!} (2\pi \delta_{\alpha\beta}) \int \kappa d\kappa (\kappa^{\alpha+\beta} |\vec{k}|^{d-j-3}) \quad (20)$$

This means that all terms with  $\alpha \neq \beta$  go to zero. This cancels a sum over  $\beta$  allowing us to write the sum over  $\alpha$  and  $\gamma$  exclusively.

$$\delta\varepsilon = \chi \sum_n \sum_{q|jm} (2\pi) \left(\frac{1}{\sqrt{2}}\right)^{2\alpha} \frac{\left(\frac{n\pi}{a}\right)^{\gamma}}{2^{\alpha} (\alpha!)^2 \gamma!} \int \kappa d\kappa (\kappa^{2\alpha} |\vec{k}|^{d-j-3}) \quad (21)$$

From the tensor paper the condition  $\alpha - \beta = m$  on the  $q$  sum implies  $m = 0$  and gives  $\chi_0 = -\frac{k_{(1)j0}^{(d)}}{8\pi^2} \sqrt{\frac{(2j+1)(j!)^2}{4\pi}}$ . Simplifying further and using  $|\vec{k}| = \sqrt{k_x^2 + k_y^2 + k_z^2} = (\kappa^2 + (\frac{n\pi}{a})^2)^{\frac{1}{2}}$  we have,[5]

$$\delta\varepsilon = \chi_0 \sum_n \sum_{q|jm} (2\pi) \left(\frac{1}{4}\right)^{\alpha} \frac{\left(\frac{n\pi}{a}\right)^{\gamma}}{(\alpha!)^2 \gamma!} \int \kappa d\kappa (\kappa^{2\alpha}) (\kappa^2 + (\frac{n\pi}{a})^2)^{\frac{d-j-3}{2}} \quad (22)$$

We now apply the transformation from array (50) and introduce regulator function  $f(\nu)$  described in array (51). The introduction of this function is simply the assertion that there exists some cutoff x-y wave vector magnitude  $\kappa_{cutoff}$  such that the energy tapers off at infinity. In one approach one could simply replace the upper integral bound of  $\infty$  with this  $\kappa_{cutoff}$  but this implies a hard, step-function like cutoff to the integral. We found that this is assuming too much about the way in which the energy falls off. So, this hard-cutoff was simply replaced by the hidden integral factor  $f(\nu)$  described in array (51).

$$\delta\varepsilon = \chi_0 \sum_n \sum_{q|jm} (2\pi) \left(\frac{1}{4}\right)^{\alpha} \frac{\left(\frac{n\pi}{a}\right)^{\gamma}}{(\alpha!)^2 \gamma!} \int \frac{d\nu}{2} (\nu - (\frac{n\pi}{a})^2)^{\alpha} (\nu)^{\frac{d-j-3}{2}} f(\nu) \quad (23)$$

We may now Taylor expand the factor  $(\nu - (\frac{n\pi}{a})^2)^\alpha$  giving the finite sum  $\sum_{k=0}^{\alpha} \frac{\alpha!}{(\alpha-k)!k!} (-\frac{n\pi}{a})^{2\alpha-k}$  as  $\alpha$  is finite.

$$\delta\varepsilon = \chi_0 \sum_n \sum_{q|jm} \pi \left(\frac{1}{4}\right)^\alpha \left(\frac{n\pi}{a}\right)^\gamma \frac{1}{(\alpha!)^2 \gamma!} \int d\nu \sum_{k=0}^{\alpha} \frac{\alpha!}{(\alpha-k)!k!} \left(-\frac{n\pi}{a}\right)^{2\alpha-k} \nu^k \nu^{\frac{d-j-3}{2}} \quad (24)$$

We may once again pull the factors independent of the integration through the integral.

$$\delta\varepsilon = \chi_0 \sum_n \sum_{q|jm} \pi \left(\frac{1}{4}\right)^\alpha \left(\frac{n\pi}{a}\right)^\gamma \frac{1}{(\alpha!)^2 \gamma!} \sum_{k=0}^{\alpha} \frac{(-1)^{\alpha-k} \alpha!}{(\alpha-k)!k!} \left(\frac{n\pi}{a}\right)^{2\alpha-2k} \int d\nu (\nu^{\frac{2k+d-j-3}{2}}) f(\nu) \quad (25)$$

Equation (52) from the appendix shows the repeated integration by parts solution to the general form  $\int f(x) x^{p/2} dx$  for integer  $p$ .

$$\delta\varepsilon = \chi_0 \sum_n \sum_{q|jm} \pi \left(\frac{1}{4}\right)^\alpha \left(\frac{n\pi}{a}\right)^\gamma \frac{1}{(\alpha!)^2 \gamma!} \sum_{k=0}^{\alpha} \frac{(-1)^{\alpha-k} \alpha!}{(\alpha-k)!k!} \left(\frac{n\pi}{a}\right)^{2\alpha-2k} \sum_{i=0}^{\infty} (-1)^i \frac{2^{i+1} (2k+d-3)!!}{(2k+d-j-3+2(i+1))!!} f^{(i)}(\nu) \nu^{\frac{2k+d-j-3+2(i+1)}{2}} \Big|_{\left(\frac{n\pi}{a}\right)^2}^{\infty} \quad (26)$$

We now apply the properties of the regulator  $f(\nu)$  that we defined in array 51 and we see that only the  $i = 0$  term of the  $i$  sum survives.

$$\delta\varepsilon = \chi_0 \sum_n \sum_{q|jm} \pi \left(\frac{1}{4}\right)^\alpha \left(\frac{n\pi}{a}\right)^\gamma \frac{1}{(\alpha!)^2 \gamma!} \sum_{k=0}^{\alpha} \frac{(-1)^{\alpha-k} \alpha!}{(\alpha-k)!k!} \left(\frac{n\pi}{a}\right)^{2\alpha-2k} \frac{2}{2k+d-j-1} \left(\frac{n\pi}{a}\right)^{2k+d-j-1} \quad (27)$$

Summation order is arbitrary and thus we may pull the  $n$  sum through the other two sums.

$$\delta\varepsilon = \chi_0 \sum_{q|jm} \frac{2\pi}{4^\alpha (\alpha!)^2 \gamma!} \sum_{k=0}^{\alpha} \frac{(-1)^{\alpha-k} \alpha!}{(\alpha-k)!k! (2k+d-j-1)} \left(\frac{\pi}{a}\right)^{2\alpha+\gamma+d-j-1} \sum_n n^{2\alpha+\gamma+d-j-1} \quad (28)$$

Finally, we use the summation rules for equation (46) defined in the tensor paper and reintroduce  $\chi_0$ .

$$\delta\varepsilon = -\frac{k_{(I)j0}^{(d)}}{8\pi^2} \sqrt{\frac{(2j+1)(j!)^2}{4\pi}} \sum_{\gamma} \left[ \frac{2\pi}{4^\alpha (\alpha!)^2 \gamma!} \sum_{k=0}^{\alpha} \frac{(-1)^{\alpha-k} \alpha!}{(\alpha-k)!k! (2k+d-j-1)} \left(\frac{\pi}{a}\right)^{2\alpha+\gamma+d-j-1} \sum_n n^{2\alpha+\gamma+d-j-1} \right]_{\alpha=\frac{1}{2}(j-\gamma)} \quad (29)$$

From the tensor paper we have that the sum  $\sum_{\gamma}$  is carried out for  $j, j-2, j-4, \dots \geq \gamma \geq 0$ . [5]

$$\delta\varepsilon = -\frac{k_{(I)j0}^{(d)}}{4\pi} \sqrt{\frac{(2j+1)(j!)^2}{4\pi}} \sum_n n^{d-1} \left(\frac{\pi}{a}\right)^{d-1} \sum_{\gamma} \frac{1}{4^{\frac{j-\gamma}{2}} \left(\frac{j-\gamma}{2}\right)! \gamma!} \sum_{k=0}^{(j-\gamma)/2} \frac{(-1)^{\frac{j-\gamma}{2}-k}}{\left(\frac{j-\gamma}{2}-k\right)! k! (2k+d-1)} \quad (30)$$

Now we may use our summation technique stated in equation 58 which gives us our final expression of,

$$\delta\varepsilon = -\frac{k_{(I)j0}^{(d)}}{4\pi} \sqrt{\frac{(2j+1)(j!)^2}{4\pi}} \zeta(1-d) \left(\frac{\pi}{a}\right)^{d-1} \sum_{\gamma} \frac{1}{4^{\frac{j-\gamma}{2}} \left(\frac{j-\gamma}{2}\right)! \gamma!} \sum_{k=0}^{(j-\gamma)/2} \frac{(-1)^{\frac{j-\gamma}{2}-k}}{\left(\frac{j-\gamma}{2}-k\right)! k! (2k+d-1)} \quad (31)$$

With the sum  $\sum_{\gamma}$  is carried out for  $\{\gamma = j-2l \geq 0, l \in \mathbb{Z}\}$ , this gives the general expression for the energy correction due to an arbitrary  $d, j, m$  Lorentz violating term. [5]

### III. EXPERIMENTAL MEASUREMENT

#### A. Proximity Force Theorem

While ideally the Casimir effect would just be measured between two parallel conducting plates as the theoretical calculation goes, in practice this is very difficult. Moving two flat surfaces within a micrometer of each other while

keeping them parallel is a virtually impossible task. However, it is possible to get a point on a sphere this close to one flat plate. Despite this difference in geometry, we can use an approximation based on this spherical-to-flat approximate geometry using the proximity force theorem. This proximity force theorem generalizes this type of approximation for parallel objects with a distance dependent potential to a spherical and flat distance dependent potential.[1] For some proximity energy  $V_p$  associated with a gently curved gap between two surfaces of variable separation  $D$  we may write,

$$V_p = \iint e(D) d\sigma + \text{corrections} \quad (32)$$

where  $e(D)$  is the energy density per unit area of two parallel interacting surfaces at separation  $D = n_r - n_L$  where  $n_R$  and  $n_L$  give the edges of the region. This is an exact formula for two flat surfaces so the corrections  $\rightarrow 0$  as the curvature of the surfaces  $\kappa \rightarrow 0$ . It is then useful to choose a mean gap surface  $\Gamma$  as is shown in figure 1.



FIG. 1: Mean Gap Surface

We may then consider  $\Gamma$  to be the domain of our distance function  $D$  with  $D = D(u, v)$  for some coordinates  $(u, v)$  on  $\Gamma$ .

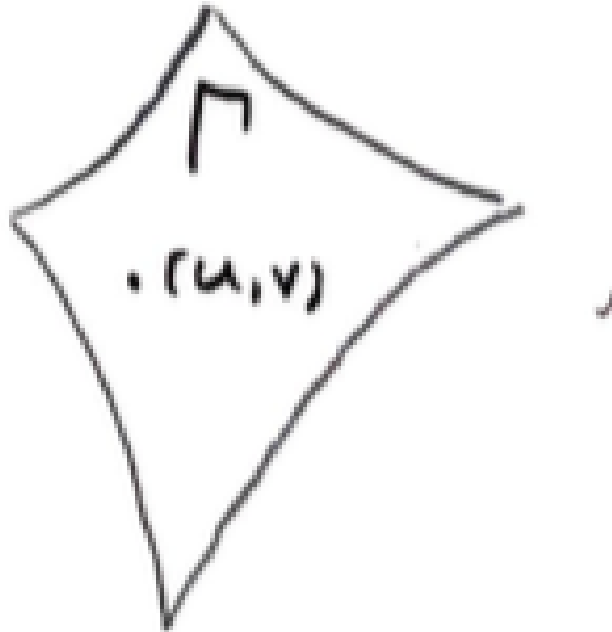


FIG. 2:  $\Gamma$  as a domain of  $D$

From here we can transform our area element  $d\sigma$  with some function of  $\Gamma$ 's geometry  $J(D)$ .

$$V_p = \int e(D)J(D)dD + \dots \quad (33)$$

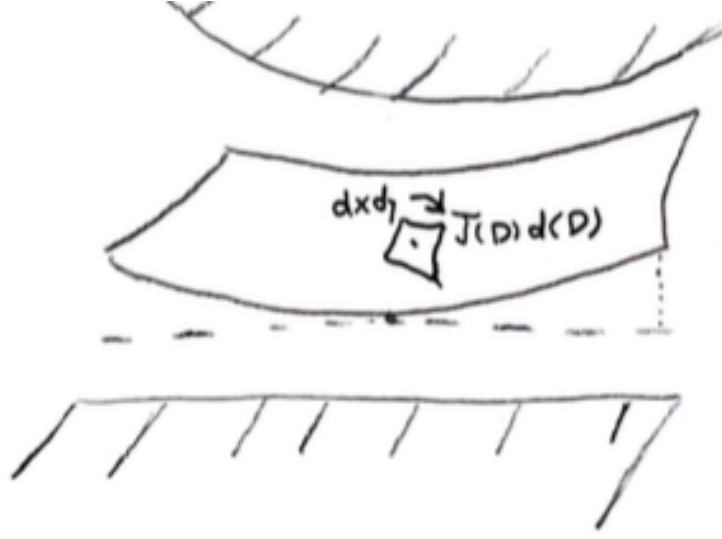


FIG. 3: Area Element transformation on  $Ga$

However this is assuming some symmetry on the surface  $\Gamma$  thus writing,

$$V_p = \int e(\beta, D)J(\alpha, D)dD + \dots \quad (34)$$

where  $\alpha$  specifies the geometry of  $\Gamma$  and  $\beta$  specifies the structure of the energy region. From here we can assess our problems particular geometry more exactly. On our surface we consider a sphere of a large radius close to a parallel plate. Since the radius of the sphere is large we may let our coordinates  $(u, v)$  on  $\Gamma$  be effectively Cartesian with  $(u, v) \rightarrow (x, y)$ . We may also rewrite  $D = n_r - n_L$  as  $D = z_r - z_L$  for a Cartesian normal direction. From equation 32 we have,

$$V_p = \int \int e(D)dx dy \quad (35)$$

on our surface  $\Gamma$ . Now we gap width  $D(x, y)$  and we may choose coordinates such that  $D = s$  for some least gap value  $s$  where  $(x, y) = (0, 0)$ . Locally this distance function may be taylor expanded with,

$$D(x, y) = s + \frac{1}{2}D_{xx}x^2 + \frac{1}{2}D_{yy}y^2 + \dots \quad (36)$$

Where  $D_{ii}$  are the second derivatives of  $D$  with respect to  $x$  and  $y$ . We may choose our  $x, y$  directions along the principal axes at the point so that our cross terms drop out as such. We may also treat these second derivatives as principal curvatures as they relate to the radii of their tangent spheres of radii  $R_x, R_y$  respectively. This gives  $D_{ii} = \frac{1}{R_i}$  We may then rewrite  $D$ ,

$$D(x, y) = s + \frac{1}{2R_x}x^2 + \frac{1}{2R_y}y^2 + \dots \quad (37)$$

We may further define  $\xi = \frac{x}{(2R_x)^{\frac{1}{2}}}$  and  $\eta = \frac{y}{(2R_y)^{\frac{1}{2}}}$ . This gives,  $D = s + \rho^2$  with  $\rho^2 = \xi^2 + \eta^2$ . Using this and transforming equation 35 we obtain,

$$V_p = 2(R_x R_y)^{\frac{1}{2}} \int \int e(D) d\xi d\eta \quad (38)$$

Transforming the integral from Cartesian to polar coordinates,

$$V_p = 2(R_x R_y)^{\frac{1}{2}} \int_0^\infty (2\pi\rho) e(D) d\rho \quad (39)$$

Transforming the integral with  $\frac{dD}{2} = \rho d\rho$  this gives,

$$V_p = 2\pi(R_x R_y)^{\frac{1}{2}} \int_{D=s}^\infty e(D) dD \quad (40)$$

Assuming that  $e(D) \rightarrow 0$  at  $\infty$  we can write,

$$V_p = 2\pi\bar{R}E(s) \quad (41)$$

where  $\bar{R} = (R_x R_y)^{\frac{1}{2}}$  is the geometric mean of  $R_x$  and  $R_y$ . To make this into a testable prediction of the force we use the relation,  $F(s) = -\frac{\partial V_p}{\partial s}$  which yields,

$$F(s) = 2\pi\bar{R}e(s) \quad (42)$$

Which when adjusted for our correction energy gives,

$$\delta F(s) = 2\pi R \delta \varepsilon(s) \quad (43)$$

where  $R$  is the radius of our sphere and  $\varepsilon(s)$  is our energy density on the Casimir plates including the energy correction calculated in the previous section.

#### IV. EXPERIMENTS: PAST, PRESENT, AND FUTURE

As I have virtually no experience with high precision experiment so I was relatively unaware of what was required of high precision experiments. The energy density of the Lorentz invariant Casimir effect goes like  $\frac{1}{a^3}$  which means the force per area goes like  $\frac{1}{a^4}$ . For the correction terms we have  $\delta\varepsilon \propto \frac{1}{a^b}$  with  $b = j + d - 1 \geq 0 + 6 - 1 = 5$  which means the largest correction to the force is  $\propto \frac{1}{a^6}$ . This is extremely tiny and the distance required to calculate the Lorentz invariant term is already on the order of fractions of a  $\mu\text{m}$ . So far, I have looked into three major experimental precedents to test my results. The experiments that have been conducted thus far would likely need to be observed over long periods of time (so the earth can spin) or placed on a turntable to verify the directional dependent effects described in this paper. For experiments measuring strictly the force dependence on plate separation, equation 43 is likely the most useful. As it is difficult to hold two flat surfaces close enough together, holding a sphere and a flat plate close and using the proximity force approximation is the standard method. However, for the proposed experiment observing the system as it rotates in time (i.e. around the sun) the following equation can be used to write the measured Lorentz violating coefficients in time. The notation here follows that in the spherical harmonics paper.[5]

$$k_{jm}^{lab} = \sum_{m'} e^{im\phi} e^{im'\omega_\oplus T_\oplus} d_{mm'}^{(j)}(-\chi) k_{jm'}^{Sun} \quad (44)$$



### A. Demonstration of the Casimir Force in the 0.6 to 6 $\mu\text{m}$ Range (1997)

This paper recognizes one of the historical issues in measurement of the Casimir Effect. This is the fact that it is extremely difficult to bring two parallel plates close enough together to measure the Casimir effect. My experiment would need the plates to be brought even closer together so the methods used in this experiment could be potentially helpful. To avoid this issue with parallel plates, the experiment used a conducting plate and a conducting sphere. The predicted energy density on the plate was then adjusted using the proximity force theorem. This is that the force between the two plates is given by  $F = 2\pi R_{\text{eff}}W(h)$ . Where  $R_{\text{eff}}$  is the effective radius of the sphere and  $W(h)$  is the energy density function, in our case  $\varepsilon$ . So, we would expect to measure  $F = 2\pi R_{\text{eff}}\varepsilon$ . Agreement with the theory within 5% was obtained in this experiment which certainly leaves enough room for the tiny effects of the Lorentz-violating terms.[4]

### B. Precision Measurement of the Casimir Force from 0.1 to 0.9 $\mu\text{m}$ (1998)

This experiment used the same methodology as the previous experiment but this time observed the effects within 1% of the accepted value. This is even closer to the size of the expected corrections proposed by this paper. Of course this means very little because experimental error does not imply new physics but rather the limitations of our equipment. This deviation simply leaves the door open for further experiment.[6]

### C. Measurement of the Casimir force between parallel metallic surfaces (2002)

This Italian experiment is notable for the fact that they were able to pull off the measurement of the Casimir Effect using parallel plates instead of using a sphere. The force was measured using a silicon cantilever coated with chromium and a similar metallic and rigid surface as the two plates. The distances tested here were in the .5-3 $\mu\text{m}$  range. However the precision of this experiment was only 15% which is much less than the previously mentioned experiments. This lack of precision may have come from the effort in the experiment to keep the two tiny plates electrically neutral. A potential difference was applied to regulate this which introduced the need for a model of this voltage and subsequently more uncertainty. An experiment like this is favorable in that the adjustments to the theory would be more minimal but the experimental precision is more difficult to regulate. As the effects we would be trying to measure are tiny, choosing the right experiment is crucial. A poor theory approximation or experimental error could both easily be large enough to absorb the effects from Lorentz violations.[2]

### D. Casimir forces on a silicon micromechanical chip (2013)

In this experiment, researchers created a micromechanical chip that could measure the casimir effect. The chip consisted of a micromechanical beam and an electrostatic actuator. The Casimir effect between two silicon components was then determined. The two micromachined elements were able to maintain a high level of parallelism as they were created in a single machining step, not created separately and then brought together. This is done by performing a dry etching on a piece of materials, creating two walls that are almost perfectly vertical. The two silicon elements were the beam and an electrode. Other integrated circuit elements were used to maintain electric neutrality on the plates and measure the Casimir Force. The difficult bit for this experiment is the difficulty of performing error analysis. The roughness of the side walls from the etching could not be directly measured. Instead, the roughness correction had to be estimated to be about 3% of the Force at the closest difference. The calculated effect was also increased up to 1.1% at the closest distance due to the assumptions that the lithographic patterns of the beam and electrode are parallel. This is perhaps a promising experiment as it combines high precision with the preserved geometry, however it is not fantastic for varying the distance between the plates.[7]

## V. CONCLUSIONS AND LOOKING FORWARD

As shown in the calculation section of this paper, a dispersion relation that breaks Lorentz symmetry in this way produces non-zero corrections to the Casimir energy between two conducting plates. However, these correction terms become progressively smaller, with only about two terms likely being within the realm of possible experimental detection. This being said, there are two main types of experimental key signatures that could be seen if Lorentz

symmetry is broken. The first would appear simply in a test of the Casimir Energy depending on plate separation as described by the parallel plate calculation and the subsequent proximity force approximation. The second would appear in an experiment done over a longer period of time where the system's plate-perpendicular axis was rotated by placing the experiment on a turntable or simply observing its change in direction over time. In both of these cases, it has become clear that the best experimental approach to measuring these potential corrections is approximating using one flat plate and one sphere. The micro-mechanical chip approach does not allow for variable separation of the Casimir cavity and the proximity force theorem is a widely accepted and used method for experimentally measuring the Casimir effect. Experiments testing Lorentz symmetry are important in modern physics for the reasons that string theory falls short. We thus far have no theory of quantum gravity that makes testable predictions at a low energy. So, we must look to the phenomenology of fields of research potentially suggested by string theory such as Lorentz violations. While the Casimir effect itself appears to be a physical phenomenon relatively valence to modern pursuits of quantum gravity, these lower energy tests of relativity potentially offer us the smoking gun we have been looking for if their predictions are measured. At the very least, measuring these Lorentz violations would point us in the right direction towards a more complete model of particle physics.

## VI. APPENDIX

### A. Mewes and Kostelecky Paper

$$\sigma = \sum_{djm} \omega^{d-4} Y_{jm}(\hat{n}) C_{djm} \quad (45)$$

This sum includes the zero-order correction combination of coefficients for Lorentz violations in the photon sector of the Standard Model Extension. Summing over all of these coefficients will give us all of the corresponding correction terms for the Lorentz-violating Casimir energy.

### B. Tensor Paper

We have,

$$Y_{jm}(n) = (-sgn(m))^m \sqrt{\frac{(2j+1)(j+m)!(j-m)!}{4\pi 2^{|m|}}} \sum_{q|jm} \frac{n_{\uparrow}^{\alpha} n_{\downarrow}^{\beta} n_z^{\gamma}}{2^{\min(\alpha,\beta)} \alpha! \beta! \gamma!} \quad (46)$$

for  $n_{\uparrow} = \frac{1}{\sqrt{2}}(n_x + in_y)$  and  $n_{\downarrow} = \frac{1}{\sqrt{2}}(n_x - in_y)$ . The  $q$  sum can be carried out with  $q = \{\alpha, \beta, \gamma\}$  with  $\alpha - \beta = m$  and summing over  $\gamma$  with  $j - |m|, j - |m| - 2, j - |m| - 4 \dots \geq \gamma \geq 0$  and  $\alpha = \frac{1}{2}(j + m - \gamma)$  and  $\beta = \frac{1}{2}(j - m - \gamma)$ .

### C. Making a Discrete Sum Over a Wavenumber Continuous for a Particle in a Large Box

Assuming a sum over some wave number  $k$ ,  $\sum_k$ , we may write,

$$\sum_k = \frac{1}{\Delta k} \sum_k \Delta k$$

Now in a large box with periodic boundary conditions, only whole numbers of wavelengths are allowed. This gives allowed wavelengths of  $\lambda = \frac{L}{n}$ . So, as wavenumber is  $k = \frac{2\pi}{\lambda}$  we have  $k = \frac{2\pi n}{L}$ . This means the difference between adjacent wavenumbers is  $\Delta k = \frac{2\pi}{L}$ . So we may write,

$$\sum_k = \left(\frac{L}{2\pi}\right) \sum_k \Delta k$$

now taking the limit as  $\Delta k \rightarrow 0$  we have,

$$\sum_k \rightarrow \left(\frac{L}{2\pi}\right) \int_k dk \quad (47)$$

#### D. $\kappa, \theta$ Transformation and Notes

Transforming  $(k_x, k_y)$  to polar coordinates gives,

$$\begin{aligned} k_x &= \kappa \cos(\theta) \\ k_y &= \kappa \sin(\theta) \\ \kappa^2 &= k_x^2 + k_y^2 \\ dk_x dk_y &= \kappa d\kappa d\theta \end{aligned} \quad (48)$$

Note also that,

$$\begin{aligned} k_{\uparrow}^{\alpha} k_{\downarrow}^{\beta} &= \left(\frac{1}{\sqrt{2}}\right)^{\alpha} (k_x + ik_y)^{\alpha} \left(\frac{1}{\sqrt{2}}\right)^{\beta} (k_x + ik_y)^{\beta} \\ &= \left(\frac{1}{\sqrt{2}}\right)^{\alpha+\beta} (\kappa \cos(\theta) + i\kappa \sin(\theta))^{\alpha} (\kappa \cos(\theta) - i\kappa \sin(\theta))^{\beta} \\ &= \left(\frac{1}{\sqrt{2}}\right)^{\alpha+\beta} (\kappa \cos(\theta) + i\kappa \sin(\theta))^{\alpha} (\kappa \cos(-\theta) + i\kappa \sin(-\theta))^{\beta} \\ &= \left(\frac{1}{\sqrt{2}}\right)^{\alpha+\beta} \kappa^{\alpha} e^{i\theta\alpha} \kappa^{\beta} e^{-i\theta\beta} \\ &= \left(\frac{1}{\sqrt{2}}\right)^{\alpha+\beta} \kappa^{\alpha+\beta} e^{i\theta(\alpha-\beta)} \end{aligned} \quad (49)$$

#### E. $\nu$ Transformation

Note the details of the following transformation,

$$\begin{aligned} \nu &= \kappa^2 + \left(\frac{n\pi}{a}\right)^2 \\ \frac{d\nu}{2} &= \kappa d\kappa \end{aligned} \quad (50)$$

#### F. Regulator Function Properties

For arbitrary regulator function  $f(\nu)$ ,

$$\begin{aligned} \lim_{\nu \rightarrow x} f^{(n)}(\nu) &= 1 \\ &= 1 \quad n = 0, x < \infty \\ &= 0 \quad n = 0, x \rightarrow \infty \\ &= 0 \quad n \neq 0 \end{aligned} \quad (51)$$

#### G. Arbitrary Function and Half Power Integral Formula

For integer  $p$  and arbitrary function  $f(x)$ ,

$$\int f(x) x^{\frac{p}{2}} dx = \sum_{k=0}^{\infty} (-1)^k \frac{2^{k+1} p!!}{(p + 2(k+1))!!} f^{(k)}(x) x^{\frac{p+2(k+1)}{2}} \quad (52)$$

## H. Riemann Zeta Function and Euler Maclaurin Formula Equivalence for our Calculation

From definition we have the Riemann Zeta function given by,

$$\zeta(q) = \sum_n n^{-q}$$

Where  $q \in \mathbb{Z}$  for our purposes. It follows then that,

$$\zeta(-q) = \sum_n n^q \quad (53)$$

Also from definition we have,

$$\zeta(-q) = (-1)^q \frac{B_{q+1}}{q+1} \quad (54)$$

for  $q \in \mathbb{Z}^-$ . Furthermore we have the Euler Maclaurin formula,

$$\sum_{i=0}^{\infty} f(i) - \int_0^{\infty} f(x)dx = \frac{f(0)}{2} - \sum_{k=1}^{\infty} \frac{B_{2k}}{(2k)!} f^{2k-1}(0) \quad (55)$$

For the purposes of removing the inconvenient infinities from our calculated energies we will use equations 53, 54, and 55 to show the equivalence of the Riemann function and Euler-Maclaurin frameworks when analyzing the sum  $\sum_{n=-\infty}^{\infty} n^s$  for  $s \in \mathbb{Z}^+$ . For the base case we could always say that  $n^s$  was an even function because we obtained it from an expression like  $\sqrt{n^{2s}} = |n|^s$  which we got away with calling  $n^s$  just as a quick shorthand. However, for the Lorentz-violating case we have correction terms that look like  $n^s = n^{s_1}|n|^{s_2}$ , which are potentially odd functions if  $n^{s_1}$  is odd. (This is the case in our work when  $\gamma$  is odd.) However, first we will address the case where  $n^s$  is even.

So, let us start by considering the zeta function approach. We will denote the sum when considered as this special zeta-sum as  $\sum_{n_\zeta}$ . First we have,

$$\sum_{n_\zeta} n^s = \sum_{n=-\infty}^{\infty} n^s$$

For  $n^s$  even and because  $n^s|_{n=0} = 0$  we may write,

$$\sum_{n_\zeta} n^s = 2 \sum_{n=0}^{\infty} n^s$$

From here we can apply our definition of the zeta function from equation 53,

$$\sum_{n_\zeta} n^s = \zeta(-s)$$

Now applying the definition from equation 54 we have,

$$\sum_{n_\zeta} n^s = \zeta(-s) = (-1)^s \frac{B_{s+1}}{s+1} \quad (56)$$

Now considering the Euler-Maclaurin approach we want to evaluate the difference between the discrete sum and the continuous sum. This clearly represents the physical significance of the finite Casimir-energy as it clearly subtracts an infinite continuously indexed value from a discretely indexed and quantized value. We start with,

$$\sum_n n^s - \int n^s dn = \sum_{n=-\infty}^{\infty} n^s - \int_{-\infty}^{\infty} n^s dn$$

As we are taking  $n^s$  to be even here and since  $n^s|_{n=0} = 0$  we can write,

$$\sum_n n^s - \int n^s dn = 2\left(\sum_{n=0}^{\infty} n^s - \int_0^{\infty} n^s dn\right)$$

Using equation 55 when then may write,

$$\sum_n n^s - \int n^s dn = \frac{n^s|_{n=0}}{2} - \sum_{k=1}^{\infty} \frac{B_{2k}}{(2k)!} (n^s)^{(2k-1)}|_{n=0}$$

From this expression we should then consider the repeated derivative  $(n^s)^{(2k-1)}|_{n=0}$ . This derivative can be written as  $\frac{d}{dn^q} n^s = \frac{s!}{(s-q)!} n^{s-q}$ . From here we see that for the  $q < s$  terms  $n^{s-q}|_{n=0} = 0$  as  $s - q > 0$ . For the  $q > s$  terms we have  $\frac{d}{dn^q} n^s = 0$  as differentiating the  $q = s$  constant term will give 0 which differentiating further will continue to give 0. So, the only term that survives the sum is the  $q = s$  term given by  $\frac{d}{dn^s} n^s = s!$ . Thus we only keep the term of the sum where  $2k - 1 = s$  or  $k = \frac{s+1}{2}$ .

$$\sum_n n^s - \int n^s dn = -\frac{B_{2(\frac{s+1}{2})}}{(2(\frac{s+1}{2}))!} s!$$

Simplifying this gives,

$$\sum_n n^s - \int n^s dn = -\frac{B_{s+1}}{(s+1)} \quad (57)$$

So, let us compare this result from Euler-Maclaurin to the Riemann result. For  $s$  is odd  $(-1)^s = -1$  so equation 56 is equivalent to equation 57. For  $s$  is even,  $s + 1$  is odd and thus both equation 56 and equation 57 are equal to 0 as odd indexed Bernoulli numbers are 0 with the exception of  $B_1$ . However  $B_1$  is the Bernoulli number for the  $s = 0$  term and  $s > 1$  as stated initially. Thus, for our needs when  $n^s$  is even and  $s \in \mathbb{Z}$  we may write,

$$\sum_{n_\zeta} n^s = \sum_n n^s - \int n^s dn = \zeta(-s) \quad (58)$$

Now looking at the case where  $n^s$  is odd we can see the following for our zeta function approach,

$$\sum_{n_\zeta} n^s = \sum_{n=-\infty}^{\infty} n^s$$

Accounting for  $n^s|_{n=0} = 0$  and rewriting the sum we see,

$$\sum_{n_\zeta} n^s = \sum_{n=0}^{\infty} n^s + \sum_{n=-\infty}^0 n^s$$

We may re-index the second sum like so,

$$\sum_{n_\zeta} n^s = \sum_{n=0}^{\infty} n^s + \sum_{n=0}^{\infty} (-n)^s$$

Now using the definition of an odd function we may write,

$$\sum_{n_\zeta} n^s = \sum_{n=0}^{\infty} n^s - \sum_{n=0}^{\infty} (n)^s$$

So,

$$\sum_{n_\zeta} n^s = 0 \quad (59)$$

Now looking at our respective Euler-Maclaurin approach we see,

$$\sum_n n^s - \int n^s dn = \sum_{n=-\infty}^{\infty} n^s - \int_{-\infty}^{\infty} n^s dn$$

The treatment of the discrete sum term holds from the previous treatment of the zeta function sum. So,

$$\sum_n n^s - \int n^s dn = - \int_{-\infty}^{\infty} n^s dn$$

Now we simply have an odd function integrated from  $-\infty$  to  $\infty$  which gives 0. So,

$$\sum_n n^s - \int n^s dn = 0 \quad (60)$$

So,

$$\sum_{n_\zeta} n^s = \sum_n n^s - \int n^s dn = 0 \quad (61)$$

for  $n^s$  is odd.

- 
- [1] J. Blocki, J. Randrup, W.J. Świątecki, and C.F. Tsang *et al.*, Proximity Forces, *Annals of Physics* **105**, 427-462 (1977).  
[2] G. Bressi, G. Carugno, R. Onofrio, and G. Ruoso *et al.*, Measurement of the Casimir Force between Parallel Metallic Surfaces, *Phys. Rev. Lett.* **88**, 041804 (2002).  
[3] V.A. Kostelecký and M. Mewes *et al.*, Astrophysical Tests of Lorentz and CPT Violations with Photons, *Astrophysical Journal Letters* **689**, L1 (2008).  
[4] S.K. Lamoreaux *et al.*, Demonstration of the Casimir Force in the 0.6 to 6  $\mu\text{m}$  Range, *Phys. Rev. Lett.* **78**, 5 (1997).  
[5] F.G. Ledesma and M. Mewes *et al.*, Spherical-harmonic Tensors, *Phys. Rev. Research* **2**, 043061 (2020).  
[6] U. Mohideen and A. Roy *et al.*, Precision Measurement of the Casimir Force from 0.1 to 0.9  $\mu\text{m}$ , *Phys. Rev. Lett.* **81**, 4549 (1998).  
[7] J. Zou, Z. Marcet, A. W. Rodriguez, M. T. H. Reid, A.P. McCauley, I.I. Kravchenko, T. Lu, Y. Bao, S.G. Johnson, H.B. Chan *et al.*, Casimir Forces on a Silicon Micromechanical Chip, *Nature Communications* **4**, 1845 (2013).